JOURNAL OF GUIDANCE, CONTROL, AND DYNAMICS
Vol. 17, No. 5, September–October 1994

Guidance Law for Hypersonic Gliders Based on Piecewise Constant Control

David G. Hull*
University of Texas at Austin, Austin, Texas 78712
and
Jean-Marie Seguin†
Aerospatiale, Les Mureaux, France

A midcourse guidance law is developed for the descent of a hypersonic glider, initially in level flight, to a fixed target on the ground. It is based on an optimal piecewise constant control (N intervals) obtained from an approximate physical model (flat Earth, exponential atmosphere, parabolic drag polar, etc). The resulting optimal control equations can be integrated either analytically or by quadrature, and the guidance algorithm requires the solution of $2N + 1$ nonlinear algebraic equations. The guidance law is implemented in a realistic glider simulation, the intercept is achieved, and final velocities within 14% of the true values are obtained for the downrange and crossranges considered.

Nomenclature

C_D = drag coefficient
C_{D_0} = coefficient of parabolic drag polar
C_L = lift coefficient
C_S = side force coefficient
g_e = acceleration of gravity at sea level, ft/s^2
h = altitude, ft
K = coefficient of parabolic drag polar
M = Mach number
m = mass, slugs
N = number of intervals
R = planet radius, ft
S_r = aerodynamic reference area, ft^2
T_g = guidance period, s
V = velocity, ft/s
v = dimensionless velocity, $-\ln(V/V_0)$
X = downrange, ft
Y = crossrange, ft
α = angle of attack, rad
β = sideslip angle, rad
β_e = density scale height, ft
γ = flight path angle, rad
ψ = heading angle, rad
ρ = atmospheric density, slugs/ft^3
ρ_e = density at sea level, slugs/ft^3

I. Introduction

IT is desired to develop a midcourse guidance law for the descent of a hypersonic glider, initially in level flight, to a fixed target on the ground while maximizing the impact velocity. The procedure employed here is to find an approximate optimal control under the assumption that the current vehicle state is known, compute its value at the current sample point, and hold it constant over the sample period. Because the optimal control equations can be integrated analytically or by quadrature for a constant control, a piecewise-constant control with N intervals is assumed.

Received May 12, 1993; presented as Paper 93-3888 at the Guidance, Navigation, and Control Conference, Monterey, CA, Aug. 9–11, 1993; revision received Nov. 5, 1993; accepted for publication Jan. 10, 1994.

*M. J. Thompson Regents Professor, Department of Aerospace Engineering and Engineering Mechanics. Associate Fellow AIAA.

†Engineer, Missions and Performances Department. Student Member AIAA.

The search for a guidance law for the three-dimensional descent of a hypersonic glider to a fixed point has been going on for some time. An initial attempt[1] reduced the problem to a turn at nearly constant altitude until the glider velocity vector is nearly in the vertical plane containing the target followed by a nearly planar descent to the target. These and related results are also contained in Refs. 2–5. Although the results of Ref. 5 have been derived for small crossranges, they can be employed for moderate crossranges.

In this paper, the approximate physical model and the corresponding optimal control problem are developed in Sec. II. Then, the optimal control results for a piecewise-constant control are presented in Sec. III. Section IV contains the corresponding results for the glider problem. The guidance algorithm is discussed in Sec. V, and simulation results are given in Sec. VI. Section VII contains the conclusions.

II. Approximate Optimal Control Problem

In setting up the approximate optimal control problem, the following assumptions are made:

a) The flat-Earth model is valid except for Loh's term,[6] which is proportional to

$$\bar{M} = \frac{2m}{\rho S_r V}\left(\frac{V}{R} - \frac{g_e}{V}\right)\cos\gamma \tag{1}$$

b) The gravity term is negligible in the $\dot{V}$ equation, and the nonaerodynamic term (1) in the $\dot{\gamma}$ equation is assumed to be constant but whose value is updated at each sample point.

c) The atmosphere is exponential, that is,

$$\rho = \rho_e e^{-h/\beta_e} \tag{2}$$

d) The drag polar is parabolic, that is,

$$C_D = C_{D_0} + K(C_L^2 + C_S^2) \tag{3}$$

where the Mach number dependent coefficients C_{D_0} and K are assumed constant over a trajectory, but like Loh's term, their values are updated at each sample point.

e) In the approximate equations of motion, the dimensionless velocity

$$v = \ln\frac{V_0}{V} \tag{4}$$

is monotonic and used as the variable of integration. The equation of motion for the time can then be discarded. Note that $v_0 = 0$, $v \geq 0$, and if the final velocity is a maximum, v_f is a minimum.

The equations of motion for flight over a nonrotating spherical Earth[7] with approximations a–e included are given in Eqs. (6–10).

With these assumptions, the optimal control problem is to find the control histories $C_L(v)$ and $C_S(v)$ that minimize the performance index

$$J = v_f = \int_0^{v_f} \mathrm{d}v \tag{5}$$

subject to the differential equations of motion

$$\frac{\mathrm{d}X}{\mathrm{d}v} = \frac{2m\cos\gamma\cos\psi}{C_D\rho S_r} \tag{6}$$

$$\frac{\mathrm{d}Y}{\mathrm{d}v} = \frac{2m\cos\gamma\sin\psi}{C_D\rho S_r} \tag{7}$$

$$\frac{\mathrm{d}\rho}{\mathrm{d}v} = -\frac{2m\sin\gamma}{\beta_e C_D S_r} \tag{8}$$

$$\frac{\mathrm{d}\gamma}{\mathrm{d}v} = \frac{C_L + \bar{M}}{C_D} \tag{9}$$

$$\frac{\mathrm{d}\psi}{\mathrm{d}v} = \frac{C_S}{C_D\cos\gamma} \tag{10}$$

the prescribed initial conditions

$$\begin{array}{lll} v_0 = 0, & X_0 = X_{0s}, & Y_0 = Y_{0s} \\ \rho_0 = \rho_{0s}, & \gamma_0 = \gamma_{0s}, & \psi_0 = \psi_{0s} \end{array} \tag{11}$$

and the prescribed final conditions (v_f free)

$$X_f = X_{fs}, \qquad Y_f = Y_{fs}, \qquad \rho_f = \rho_{fs} \tag{12}$$

where the subscript s denotes a specified value. Because of the nature of the vehicle and the actual initial conditions, no heating constraint is needed.

If C_L and C_S are constant, Eqs. (8–10) can be integrated analytically, and the integration of Eqs. (6) and (7) reduces to quadrature. For this reason, it has been decided to investigate the case of optimal piecewise-constant control and apply it to this problem. The number N of control segments between the sample point and the final point is held constant. This work was motivated by the finite element approach,[8] which uses low-order integration but exact equations of motion.

III. Optimal Piecewise Constant Control

The general statement of this optimal control problem is to find the N constant controls u_i and the final time t_{N+1} that minimize the performance index

$$J = \phi(t_{N+1}, x_{N+1}) + \sum_{i=1}^{N} \int_{t_i}^{t_{i+1}} L(t, x, u_i)\mathrm{d}t \tag{13}$$

subject to the N differential constraints

$$\dot{x} = f(t, x, u_i), \qquad t_i \le t \le t_{i+1} \tag{14}$$

the prescribed initial conditions

$$t_1 = t_{1s}, \qquad x_1 = x_{1s} \tag{15}$$

and the prescribed final conditions

$$\psi(t_{N+1}, x_{N+1}) = 0 \tag{16}$$

For equal control intervals,

$$t_i = \frac{i-1}{N} t_{N+1} \tag{17}$$

and the states are required to be continuous at each corner, that is,

$$x_{i,a} = x_{i,b}, \qquad i = 2, \ldots, N \tag{18}$$

where a refers to just after the corner and b, to just before the corner.

By applying the standard methods of optimal control theory,[9] the conditions for a minimum can be derived in a straightforward manner. After the constraints are adjoined to the performance index, the Hamiltonian H and the endpoint function G are defined as

$$H_i = L(t, x, u_i) + \lambda^T f(t, x, u_i), \qquad t_i \le t \le t_{i+1} \tag{19}$$

$$G = \phi(t_{N+1}, x_{N+1}) + \nu^T \psi(t_{N+1}, x_{N+1}) \tag{20}$$

Then, standard variational techniques lead to the following conditions over each constant control interval:

$$\dot{x} = f(t, x, u_i) \tag{21}$$

$$\dot{\lambda} = -H_x^T(t, x, u_i, \lambda) \tag{22}$$

$$0 = \int_{t_i}^{t_{i+1}} H_{u_i}^T \,\mathrm{d}t. \tag{23}$$

These segments are put together by satisfying the initial conditions

$$t_1 = t_{1s}, \qquad x_1 = x_{1s} \tag{24}$$

the corner conditions

$$t_i = \frac{i-1}{N} t_{N+1}, \qquad x_{i,a} = x_{i,b}, \qquad \lambda_{i,a} = \lambda_{i,b} \tag{25}$$

and the final conditions

$$\psi(t_{N+1}, x_{N+1}) = 0 \tag{26}$$

$$\lambda_{N+1} = G_{x_{N+1}}^T \tag{27}$$

$$G_{t_{N+1}} + H_{N+1} + \sum_{i=2}^{N} (H_{i,b} - H_{i,a}) \frac{i-1}{N} = 0 \tag{28}$$

If the Hamiltonian is explicitly independent of the time, the first integral $H = \text{const} = H_{i,a} = H_{i+1,b}$ exists over each constant control interval and allows Eq. (28) to be rewritten as

$$G_{t_{N+1}} + \frac{1}{N} \sum_{i=1}^{N} H_i = 0 \tag{29}$$

where H_i now denotes the value of H over the ith interval.

IV. Application to Glider Problem

First, because there are two controls and three final conditions, the number of control intervals must be $N \ge 2$. Second, since L and f do not explicitly contain v, the first integral exists over each interval. Finally, the Hamiltonian over each interval and the end point function are given by

$$\begin{aligned} H_i = 1 &+ \lambda_X \frac{2m\cos\gamma\cos\psi}{C_{D_i}\rho S_r} + \lambda_Y \frac{2m\cos\gamma\sin\psi}{C_{D_i}\rho S_r} \\ &- \lambda_\rho \frac{2m\sin\gamma}{\beta_e C_{D_i} S_r} + \lambda_\gamma \frac{C_{L_i} + \bar{M}}{C_{D_i}} - \lambda_\psi \frac{C_{S_i}}{C_{D_i}\cos\gamma} \end{aligned} \tag{30}$$

$$\begin{aligned} G = \nu_X &(X_{N+1} - X_{N+1_s}) + \nu_Y (Y_{N+1} - Y_{N+1_s}) \\ &+ \nu_\rho (\rho_{N+1} - \rho_{N+1_s}) \end{aligned} \tag{31}$$

The equations of motion can be integrated over each interval in terms of v, but the results are more easily expressed in terms of γ. In doing so, the term $C_{L_i} + \bar{M}$ appears in the denominator. Although $C_{L_i} + \bar{M} \neq 0$ in this study, it could happen in other situations. If so, equations for $C_{L_i} + \bar{M} = 0$ must be derived.

Integration of Eqs. (8–10) gives

$$\gamma = \gamma_i + \frac{C_{L_i} + \bar{M}}{C_{D_i}}(v - v_i) \tag{32}$$

$$\rho = \rho_i + \frac{2m(\cos\gamma - \cos\gamma_i)}{\beta_e(C_{L_i} + \bar{M})S_r} \tag{33}$$

$$\psi = \psi_i + \frac{C_{S_i}}{C_{L_i} + \bar{M}} \ln\frac{\tan(\pi/4 + \gamma/2)}{\tan(\pi/4 + \gamma_i/2)} \tag{34}$$

whereas Eqs. (6) and (7) lead to

$$\frac{dX}{d\gamma} = \beta_e \frac{\cos\left(\psi_i + \frac{C_{S_i}}{C_{L_i} + \bar{M}} \ln\frac{\tan(\pi/4 + \gamma/2)}{\tan(\pi/4 + \gamma_i/2)}\right)\cos\gamma}{\cos\gamma - \cos\gamma_i + (\beta_e(C_{L_i} + \bar{M})S_r\rho_i)/2m} \tag{35}$$

$$\frac{dY}{d\gamma} = \beta_e \frac{\sin\left(\psi_i + \frac{C_{S_i}}{C_{L_i} + \bar{M}} \ln\frac{\tan(\pi/4 + \gamma/2)}{\tan(\pi/4 + \gamma_i/2)}\right)\cos\gamma}{\cos\gamma - \cos\gamma_i + (\beta_e(C_{L_i} + \bar{M})S_r\rho_i)/2m} \tag{36}$$

and can be integrated by quadrature.

The multipliers λ are continuous over the whole trajectory and satisfy the differential equations

$$\frac{d\lambda_X}{dv} = 0 \tag{37}$$

$$\frac{d\lambda_Y}{dv} = 0 \tag{38}$$

$$\frac{d\lambda_\rho}{dv} = \frac{2m\cos\gamma}{\rho^2 C_D S_r}(\lambda_X \cos\psi + \lambda_Y \sin\psi) \tag{39}$$

$$\frac{d\lambda_\psi}{dv} = \frac{2m\cos\gamma}{\rho C_D S_r}(\lambda_X \sin\psi - \lambda_Y \cos\psi) \tag{40}$$

where λ_γ will be obtained from the first integral.

Equations (37) and (38) give

$$\lambda_X = C_1 \tag{41}$$

$$\lambda_Y = C_2 \tag{42}$$

and Eq. (40) combined with Eqs. (6) and (7) leads to

$$\lambda_\psi = C_1 Y - C_2 X + C_3 \tag{43}$$

Finally, Eq. (39) can be written as

$$\frac{d\lambda_\rho}{d\gamma} = \frac{\beta_e^2(C_{L_i} + \bar{M})S_r}{2m} \times \left\{ \lambda_X \frac{\cos\gamma\cos\left(\psi_i + \frac{C_{S_i}}{C_{L_i} + \bar{M}} \ln\frac{\tan(\pi/4 + \gamma/2)}{\tan(\pi/4 + \gamma_i/2)}\right)}{[\cos\gamma - \cos\gamma_i + (\beta_e(C_{L_i} + \bar{M})S_r\rho_i)/2m]^2} + \lambda_Y \frac{\cos\gamma\sin\left(\psi_i + \frac{C_{S_i}}{C_{L_i} + \bar{M}} \ln\frac{\tan(\pi/4 + \gamma/2)}{\tan(\pi/4 + \gamma_i/2)}\right)}{[\cos\gamma - \cos\gamma_i + (\beta_e(C_{L_i} + \bar{M})S_r\rho_i)/2m]^2} \right\} \tag{44}$$

and, since λ_X and λ_Y are constant, integrated by quadrature.

Over one interval, Eq. (43) can be expressed as

$$\Delta(\lambda_\psi)_i = \Delta Y_i \lambda_X - \Delta X_i \lambda_Y \tag{45}$$

where, if i refers to a corner,

$$\Delta(\cdot)_i = (\cdot)_{i+1} - (\cdot)_i \tag{46}$$

Next, Eq. (43) can be integrated and combined with Eq. (32) to give

$$(\Delta\lambda_\rho)_i = g_1(\rho_i, \gamma_i, \psi_i, C_{L_i}, C_{S_i}, v_i, v_{i+1})\lambda_X + g_2(\rho_i, \gamma_i, \psi_i, C_{L_i}, C_{S_i}, v_i, v_{i+1})\lambda_Y \tag{47}$$

Finally, λ_γ over each interval can be obtained from the first integral $H_i = \text{const}$, that is,

$$\lambda_\gamma = (H_i - 1)\frac{C_{D_i}}{C_{L_i} + \bar{M}} - \frac{2m\cos\gamma}{(C_{L_i} + \bar{M})\rho S_r}(\lambda_X \cos\psi + \lambda_Y \sin\psi) + \lambda_\rho \frac{2m\sin\gamma}{\beta_e(C_{L_i} + \bar{M})S_r} - \lambda_\psi \frac{C_{S_i}}{(C_{L_i} + \bar{M})\cos\gamma} \tag{48}$$

The next step is to apply the stationarity conditions (23). For C_{L_i}, the following result is obtained:

$$\int_{v_i}^{v_{i+1}} \lambda_\gamma dv + 2KC_{L_i}(1 - H_i)\Delta v_i = 0 \tag{49}$$

If Eq. (48) is combined with the equations of motion and integrated by parts over the interval, it is seen that

$$\int_{v_i}^{v_{i+1}} \lambda_\gamma\, dv = -\frac{C_{D_i}}{C_{L_i} + \bar{M}}[(1 - H_i)\Delta v_i + \Delta(\lambda_\rho\rho)_i + \Delta(\lambda_\psi\psi)_i - P_i] \tag{50}$$

where

$$P_i = \int_{v_i}^{v_{i+1}} \frac{2m\cos\gamma}{C_{D_i}\rho S_r}(\lambda_X \sin\psi - \lambda_Y \cos\psi)\psi\, dv \tag{51}$$

can be obtained by quadrature. Hence, the stationarity condition for C_{L_i} becomes

$$0 = (1 - H_i)\left(2KC_{L_i} - \frac{C_{D_i}}{C_{L_i} + \bar{M}}\right)\Delta v_i - \frac{C_{D_i}}{C_{L_i} + \bar{M}}[\Delta(\lambda_\rho\rho)_i + \Delta(\lambda_\psi\psi)_i - P_i] \tag{52}$$

The equivalent condition for C_{S_i} is given by

$$0 = 2(1 - H_i)KC_{S_i}\Delta v_i + \frac{C_{D_i}}{C_{S_i}}[\Delta(\lambda_\psi\psi)_i - P_i] \tag{53}$$

Equations (52) and (53) must hold over each interval and represent $2N$ equations.

Finally, the boundary conditions are the initial conditions

$$t_1 = t_{1s}, \qquad x_1 = x_{1s} \tag{54}$$

and the final conditions

$$X_{N+1} = X_{N+1,s} \tag{55}$$

$$Y_{N+1} = Y_{N+1,s} \tag{56}$$

$$\rho_{N+1} = \rho_{N+1,s} \tag{57}$$

$$\sum_{i=1}^{N} H_i = 0 \tag{58}$$

$$\lambda_{\gamma,N+1} = \lambda_{\psi,N+1} = 0 \tag{59}$$

V. Guidance Algorithm

The solution process begins with a guess of the final dimensionless velocity and the control histories, that is,

$$v_{N+1}, C_{L_1}, \ldots, C_{L_N}, C_{S_1}, \ldots, C_{S_N} \tag{60}$$

which are all physical quantities. Then, the dimensionless velocity at each corner is given by

$$v_i = \frac{i-1}{N} v_{N+1} \tag{61}$$

and Eq. (32) leads to γ_i. Next, Eqs. (33–36) provide the states x_i at each node (corners plus final point). Note that the final conditions (55–57) are not satisfied.

The next step in the solution process is to solve for λ_X, λ_Y, and $\lambda_{\rho,N+1}$, since $\lambda_{\gamma,N+1}$ and $\lambda_{\psi,N+1}$ are known to be zero. Suppose that these quantities are known. Then, from Eqs. (45) and (47), it is seen that

$$\lambda_{\psi,i} = \lambda_{\psi,N+1} - \sum_{j=i}^{N} (\Delta X_j \lambda_X + \Delta Y_j \lambda_Y) \tag{62}$$

$$\lambda_{\rho,i} = \lambda_{\rho,N+1} - \sum_{j=i}^{N} (g_{1,j} \lambda_X + g_{2,j} \lambda_Y) \tag{63}$$

At this point, H_i is computed from Eq. (30) at the right-hand side of a control interval and used at the left-hand side (H_i = const) to compute $\lambda_{\gamma,i}$, from Eq. (48). Hence, knowing λ_X, λ_Y and $\lambda_{\rho,N+1}$ leads to the multipliers and H at each node. To solve for these unknown multipliers, it is noted that Eq. (29) can be rewritten as

$$\sum_{i=1}^{N} H_i = 0 \tag{64}$$

and the stationarity conditions (52) and (53), over the last interval, form a linear system in λ_X, λ_Y, and $\lambda_{\rho,N+1}$, so they can easily be computed.

At this point, the equations that are not satisfied are the final conditions (55–57), the first $N-1$ stationarity conditions (52), and the first $N-1$ stationarity conditions (53). Hence, there are $2N+1$ equations for calculating the $2N+1$ unknowns (60). The solution is accomplished by Newton's method.

These calculations are performed at each sample point, and C_{L_1} and C_{S_1} are held constant over the sample period. At the next sample point, the results obtained at the previous sample point are used as the initial guess. At the first point, a table would be provided for the guess of the unknowns.

VI. Guidance Results

The proposed guidance algorithm has been applied to the flight of a realistic hypersonic glider for the following boundary conditions:

$$X_1 = 0 \text{ nm}, \quad Y_1 = 0 \text{ nm}, \quad h_1 = 100{,}000 \text{ ft}$$
$$V_1 = 11{,}300 \text{ ft/s}, \quad \gamma_1 = 0, \quad \psi_1 = 0$$
$$X_{N+1} = 80 \text{ nm}, \quad Y_{N+1} = 0, 40, 80 \text{ nm}, \quad h_{N+1} = 0 \text{ ft}$$

The physical model involves a nonrotating spherical Earth, a standard atmosphere, and wind-tunnel aerodynamic data. Vehicle controls are angle of attack α and sideslip angle β. The same model is used to generate optimal open-loop trajectories with a nonlinear programming code (piecewise linear control assuming six control nodes), which are taken as references for the guidance law.

The parameters employed in the guidance law are given by

$$m = 15.52 \text{ slugs}, \quad S_r = 1.5 \text{ ft}^2$$
$$\rho_e = 2.377 \times 10^{-3} \text{ slug/ft}^3, \quad \beta_e = 23{,}800 \text{ ft}$$

Obtained from curve fitting the wind-tunnel data, $C_{D_0}(M)$ and $K(M)$ are determined at each sample point by a table look-up. Commanded C_L and C_S are converted to α and β by table look-up of $C_{L_\alpha}(M)$ and $C_{L_\beta}(M)$, $C_{L_{\beta^2}}(M)$. These values can be seen in Table 1. Typically, 30 points are used for the quadrature integration over the whole trajectory.

The performance of the guidance law can be described by the vehicle state when hitting the ground (X_f, Y_f) and the final velocity V_f. All trajectories hit the ground within 0.01 nm of the target, and these results can be improved by switching to a terminal guidance scheme such as proportional navigation before impact. Values of the final velocity are shown in Table 2 for a sample period of 1.0 s and several values of N (number of control intervals). For comparison, velocities are presented for the open-loop optimal trajectories (denoted Ref.). Whereas $N = 2$ gives excellent results for zero crossrange, the number of intervals for good performance increases with crossrange. For the crossranges selected, $N = 4$ does well overall.

Additional guidance results and their corresponding reference values are presented for $N = 4$ in the sharp-turn case (80 nm crossrange). Figure 1 shows the angle of attack vs time. Note that α goes to zero at the impact point, as it should. Figure 2 shows that the sideslip angle is nearly linear. Figures 3 and 4 give respectively altitude vs time and the ground track for $N = 4$. Figure 3 shows that $N = 4$ attempts to capture the skip. In general, it can be shown that the curves approach, as N increases, a limit fairly close to the optimal curve.

Table 1 Aerodynamic model

M	C_{D_0}	K	C_{L_α}	C_{S_β}	$C_{S_{\beta^2}}$
2	0.345	0.285	2.65	−2.34	−5.09
4	0.154	0.346	2.57	−2.38	−3.42
6	0.104	0.404	2.49	−2.35	−2.61
8	0.084	0.456	2.43	−2.34	−2.13
10	0.075	0.501	2.40	−2.32	−1.81
12	0.070	0.542	2.37	−2.31	−1.57

Table 2 Final velocity, ft/s

N	$\Delta Y = 0$ nm	$\Delta Y = 40$ nm	$\Delta Y = 80$ nm
2	7251	4697	2307
3	7246	4920	2742
4	7245	4994	2950
5	7246	5035	3057
Ref.	7280	5130	3440

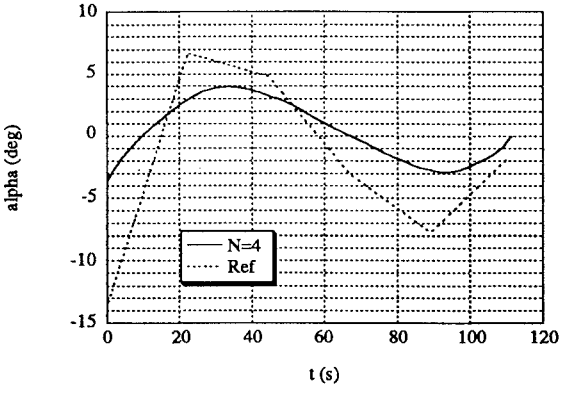

Fig. 1 Angle of attack vs time.

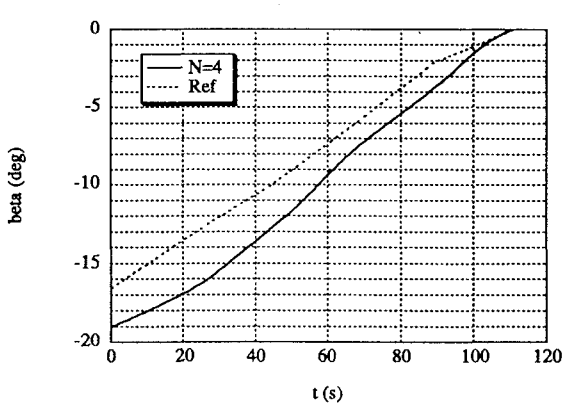

Fig. 2 Sideslip angle vs time.

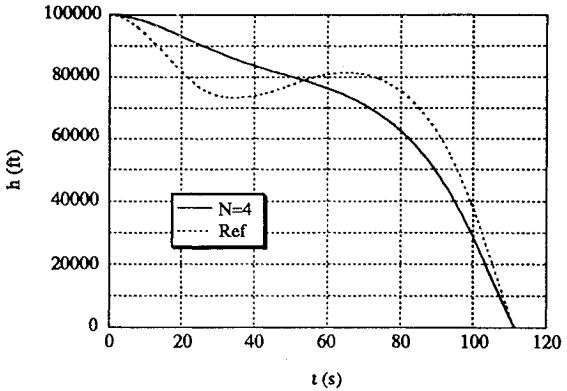

Fig. 3 Altitude vs time.

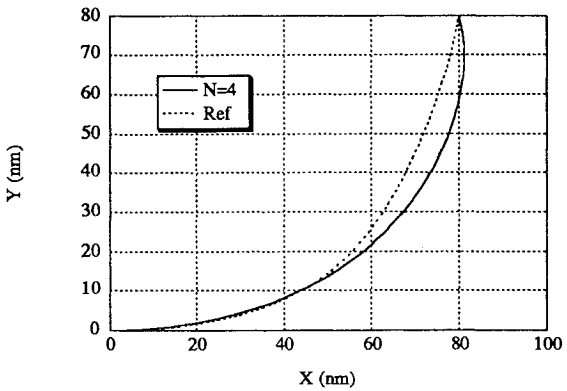

Fig. 4 Crossrange vs downrange.

The guidance law described in Ref. 5 has also been applied to the glider problem. Although that guidance law was developed for small crossranges, it gives guidance commands in the right direction and gets better as the turn progresses. The results are $V_f = 7192$ ft/s for $Y_f = 0$ nm and $V_f = 4950$ ft/s for $Y_f = 40$ nm. The guidance law as coded cannot handle $Y_f = 80$ nm. However, Ref. 5 only requires the solution of one nonlinear algebraic equation. Thus, the price to pay for performing sharp turns and getting better velocities is the resolution of a higher number of equations ($2N + 1$ instead of 1).

VII. Discussion and Conclusions

A guidance law has been developed that enables a hypersonic glider, initially in level flight, to maneuver from a given position and velocity to a fixed target on the ground with a maximum impact speed. Because most of the approximate vehicle equations of motion can be integrated analytically for constant controls, an optimal piecewise-constant control has been employed. At each sample point, the vehicle state is taken from the navigation unit; the optimal piecewise-constant control (N segments) is computed, and the first segment controls are applied to the vehicle over the sample period. The computational process involves several quadrature integrations and the solution of a system of $2N + 1$ nonlinear algebraic equations by Newton's method.

This midcourse guidance law has been tested in a realistic vehicle simulation and produces good final velocities when compared with the "true" optimal velocities. Although the performance of the guidance law increases with the number of control segments, $N = 4$ gives final velocities within 14% of the true optimal velocities for the crossranges considered.

References

[1]Eisler, G. R., "Maximum-Terminal-Velocity Guidance for a Hypersonic Glider," Ph.D. Dissertation, Univ. of Texas at Austin, Austin, TX, May 1986.

[2]Eisler, G. R., and Hull, D. G., "Optimal Descending, Hypersonic Turn to a Heading," *Journal of Guidance, Control, and Dynamics*, Vol. 10, 1987, pp. 255–261.

[3]Eisler, G. R., and Hull, D. G., "Maximum Terminal Velocity Turns at Nearly Constant Altitude," *Journal of Guidance, Control, and Dynamics*, Vol. 11, 1988, pp. 131–136.

[4]Eisler, G. R., and Hull, D. G., "Guidance Law for Planar Hypersonic Descent to a Point," *Journal of Guidance, Control, and Dynamics*, Vol. 16, 1993, pp. 400–402.

[5]Eisler, G. R., and Hull, D. G., "Guidance Law for Hypersonic Descent to a Point," *Journal of Guidance, Control, and Dynamics*, Vol. 17, 1994, pp. 649–654.

[6]Loh, W. H. T., *Re-entry and Planetary Entry Physics and Technology*, Vol. 1, Springer-Verlag, New York, 1968.

[7]Miele, A., *Flight Mechanics*, Vol. I: *Theory of Flight Paths*, Addison-Wesley, Reading, MA, 1962.

[8]Hodges, D. H., Bless, R. R., Calise, A. J., and Leung, M., "Finite Element Method for Optimal Guidance of an Advanced Launch Vehicle," *Journal of Guidance, Control, and Dynamics*, Vol. 15, 1992, pp. 664–671.

[9]Bryson, A. E., and Ho, Y. C., *Applied Optimal Control*, Hemisphere, New York, 1975.